Hall-Effect Studies in Zinc and Cadmium

G. S. LANE, A. S. HUGLIN, AND J. STRINGER*
Department of Metallurgy, University of Liverpool, Liverpool, England
(Received 27 February 1964)

Determinations have been made of the two independent components of the Hall vector for Zn at 78 and 297°K, and for Cd at 297°K using a high-sensitivity dc technique on rectangular single-crystal sheet specimens. The effect of possible errors in the measured angles between the experimental and the crystallographic coordinate systems has been calculated, and it is suggested that this is the major source of spread in the results. Small variations in the purity of the Zn had no effect on the Hall coefficient. Heat treatment of the specimen assembly produced an alteration in the Hall coefficient which eventually approached a steady value, but the sign and magnitude of the alteration was different for each crystal. Pole figures for a number of polycrystalline samples have been determined, and a process of numerical integration has been used to predict the Hall coefficient from the single-crystal data. In the case of zinc the agreement with experiment is good, but for cadmium the predicted Hall coefficient is significantly greater than the experimental value. It is suggested that this is due to short-circuiting of the Hall field by adjacent grains. The Hall coefficients of rolled polycrystalline Zn and Cd have been determined and show a systematic variation with the angle at which the specimen is cut from the sheet. An explanation of this variation is given on the basis of the asymmetry of the pole figure.

INTRODUCTION

IN discussing galvanomagnetic effects in anisotropic materials, it is necessary to adopt a definition of the Hall effect which clearly distinguishes it from the change in resistance due to a magnetic field. For isotropic materials at room temperature we may write

$$\mathbf{E}=\rho\mathbf{J}+R\mathbf{B}\times\mathbf{J}, \tag{1}$$

where $\mathbf{E}$ is the electric field, $\mathbf{J}$ is the current density, $\mathbf{B}$ is the magnetic induction, ρ is the resistivity, and R is the Hall coefficient. The second term in (1) is the Hall field, and it is normal to both the current density and the magnetic field. In anisotropic media Eq. (1) does not hold, but to facilitate comparisons between various materials it is desirable to retain in a more genera- expression the characteristic properties of $R\mathbf{J}\times\mathbf{B}$. Following Logan and Marcus[1] we choose to adopt the conl vention that the Ohmic field is

$$\tfrac{1}{2}[\mathbf{E}(\mathbf{B})+\mathbf{E}(-\mathbf{B})] \tag{2}$$

and the Hall field is

$$\tfrac{1}{2}[\mathbf{E}(\mathbf{B})-\mathbf{E}(-\mathbf{B})]. \tag{3}$$

As a result of this definition, the Hall field reverses its direction on reversing the direction of the applied magnetic field, while the Ohmic field does not. Neither term changes its magnitude on this reversal. Further, the Hall field vanishes when $\mathbf{B}=0$.

This choice is based on a calculation of Casimir,[2] who showed that, for an anisotropic material, if the vectors are resolved into components in any convenient rectangular coordinate system

$$E_i=\textstyle\sum_j \rho_{ij}J_j+(\mathbf{r}\times\mathbf{J})_i, \tag{4}$$

where the ρ_{ij} are functions of $\mathbf{B}$ such that

$$\rho_{ij}(\mathbf{B})=\rho_{ij}(-\mathbf{B}),$$

while

$$\mathbf{r}(\mathbf{B})=-\mathbf{r}(-\mathbf{B}).$$

The vector $\mathbf{r}$ is called the Hall vector. In deriving (4), Casimir neglected the interaction of thermal and galvanomagnetic effects. Kohler[3] analyzed the limitations imposed by crystal symmetry on the Hall vector. Writing

$$r_i=\textstyle\sum_j R_{ij}B_j, \tag{5}$$

we choose the coordinate system so that one axis is parallel to the hexad axis of symmetry in the hexagonal close-packed system, and the other two are parallel to mutually perpendicular directions in the basal plane. In this case, the matrix R is diagonal, and symmetry considerations together with the Onsager relationships indicate that only two of the diagonal terms are independent. We label these R_1 and R_2 and adopt the convention that R_1 is the Hall coefficient when the magnetic induction is parallel to the hexad axis.

Roesch and Willens[4] have recently noted that the large variation in the published values of the Hall coefficient for polycrystalline samples of α titanium can be interpreted in terms of the variation in the texture of the specimens and the consequently varying contributions of R_1 and R_2. The analysis is incomplete however, because of the lack of single-crystal data. In this investigation the Hall constants for polycrystalline samples of zinc and cadmium have been measured, and compared with the results predicted from the observed texture and the values of R_1 and R_2 measured for single crystals. Determinations of R_1 and R_2 have been made for both zinc and cadmium at liquid nitrogen and room temperatures by Noskov.[5] R_1 and R_2 for zinc at liquid-

* Present address: Metals Science Group, Battelle Memorial Institute, Columbus, Ohio.
[1] J. K. Logan and J. A. Marcus, Phys. Rev. 88, 1234 (1952).
[2] H. B. G. Casimir, Rev. Mod. Phys. 17, 343 (1945).
[3] M. Kohler, Ann. Physik 20, 878 (1934).
[4] L. Roesch and R. H. Willens, J. Appl. Phys. 34, 2159 (1963).
[5] M. M. Noskov, Zh. Eksperim. i Teor. Fiz. 8, 717 (1938).

nitrogen temperature have also been determined by Logan and Marcus. The results show scatter (Table I) and the values of the coefficients, especially for cadmium, where measurements have been confined to three crystals only, cannot be taken as being firmly established.

EXPERIMENTAL MATERIALS AND TECHNIQUE

The single crystals were grown in reactor-grade graphite split molds by a modified Bridgman technique from metal of nominal 99.999% purity supplied by Messrs. Light Ltd. The polycrystalline samples were prepared in the main from the same material, but to evaluate the effect of purity some specimens prepared from material of nominal 99.99% purity were studied.

The single crystals as grown measured approximately $10\times1\times0.05$ cm. Specimens were cut from these crystals using an acid saw with a chromic acid solution. The crystals were extremely soft; some of the cadmium specimens would bend under their own weight if held at one end. This made it very difficult to avoid twinning the crystals at some stage during the preparation of the specimens and mounting them in the measuring apparatus. Fortunately, the twins could easily be seen with the naked eye on the bright etched metal surface, and the back reflection Laue technique used to determine the specimen orientation was an additional check. All twinned specimens were rejected. Figure 1 shows the orientations of the specimens studied.

The polycrystalline specimens were rolled to 0.020-in. sheet at room temperature on a two-high 6 in. mill. Since both zinc and cadmium of this purity recrystallize at room temperature, this is, in fact, hot rolling; but the recrystallization texture for these metals is the same as the cold-rolled texture. In order to produce materials with different texture, some sheets were cross rolled, the sheet being rotated through 90° between each pass.

The specimen holder for the Hall effect measurements was constructed from $\frac{1}{2}$-in. diam Perspex rod for maximum rigidity. The current leads were soldered to copper screw clamps, which were clamped to the ends of the specimen. In some cases indium wire was used to improve the contact and reduce contact noise in the specimen current. The upper clamp was set in the Perspex holder and the lower was free to move along a vertical guide rod, to eliminate as far as possible strains being introduced into the specimen by differential expansion during heating and cooling.

The Hall field in the specimen was measured using a two-probe method, rather than the three-probe method used by Logan[1] and by Roesch,[4] partly to avoid loops in the magnetic field and partly to avoid introducing angular errors. The two-probe method requires accurate alignment of the Hall probes, and has the disadvantage that the observed signal includes a resistive drop due to inevitable misalignment of the probes as well as the Hall signal. The signal is thus very sensitive to variations in the specimen current. Various methods of current stabilization were used, and various methods of backing out the resistive drop, with only moderate success. Finally, a Tinsley constant current unit type-5390 was used. This supplied currents of 0.5, 1.0, 1.5, and 2.0 A accurate to 1 part in 10^6. The current was monitored with a standard resistor and a Cambridge potentiometer, but, in fact, this proved unnecessary.

TABLE I. Hall coefficients R_H (10^{-12} Ω cm G^{-1}), single crystals.

Material	R_1 288°K	R_1 77°K	R_2 288°K	R_2 77°K
Zn 1 Noskov	1.44	1.87	0.04	0.16
2	1.41	1.94	...	...
3	1.43	...	0	...
4	1.43	2.01	−0.06	0.18
5	1.44	1.86	−0.025	0.19
6	1.4	...	...	...
Zn 1 Logan	...	2.5	...	...
2	...	1.8	...	0.21
3	...	0.1	...	...
Cd 1 Noskov	1.20	1.66	0.11	0.38
2	1.45	...	...	...
3	1.32	1.74	0	0.27

The Hall probes were 0.005-in.-diam copper wire, and were spot welded to the specimen by touching the wire to the specimen and discharging a condenser through the junction. The weld was then consolidated with several further discharges. This method produced robust junctions of very small extent, and made it relatively simple to achieve good probe alignment. After welding, the Hall leads were cemented to the specimen holder and twisted together to avoid induction effects.

A Newport type-D 8-in. electromagnet with water-cooled coils with a 4-cm gap was used. The current supply was a 20-kW motor generator with an output smoothed to 1 part in 10^5. The maximum field obtained with this assembly was 18.6 kG. The smoothing on the magnet supply proved to be inadequate, and the magnet ripple was the most important source of noise. This noise was backed off with a signal from a search coil cemented to one of the pole faces.

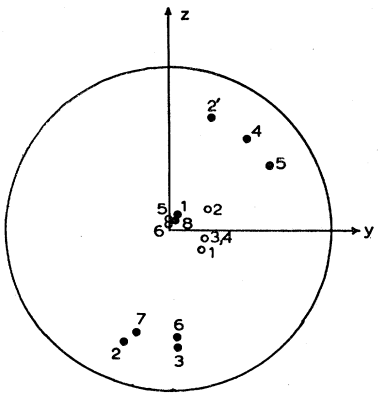

FIG. 1. Stereographic projection of specimen (0001) poles on the yz plane. Open circles-Cd. Shaded circles-Zn.

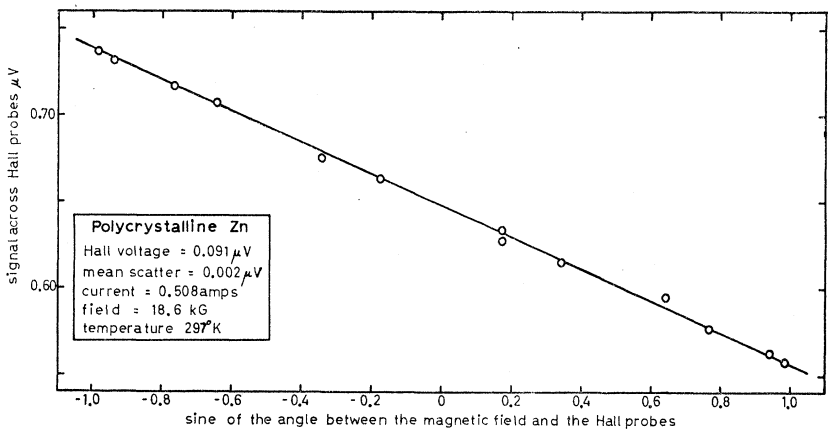

FIG. 2. An experimental curve.

The Hall signal was measured with a Tinsley Diesselhorst Thermo-electric-free potentiometer. The null signal from this was amplified with a Tinsley photocell amplifier, and finally recorded on a Kipp microvolt recorder. Shielding and earthing of the measuring circuit proved to be critical, but eventually the technique could reproducibly measure potentials within an accuracy of $\pm 5\times 10^{-9}$ V. With care, the accuracy was even better. Figure 2 shows an experimental curve obtained under good conditions. The scatter about the mean line is approximately 2×10^{-9} V, which is the magnitude of the calculated Johnson noise in the specimen circuit.

The magnet was rotated through 360° with measurements being taken every 30°. In all cases the Hall signal varied sinusoidally with magnet azimuth. In some cases a regression formula was used to fit the best sine curve to the data, but because of the small scatter this was not significantly better than the best curve fitted by direct inspection of the results. The Hall voltage was linear with both current and field in all these experiments.

The distribution of orientations of the grains in the polycrystalline specimens were determined using a Schulz goniometer[6] with a Geiger-Muller counter and a rate meter. The rate meter curve was used to plot a pole figure.

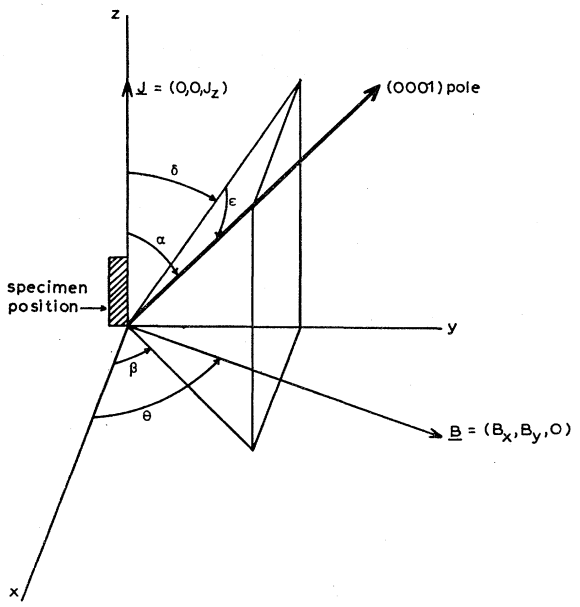

FIG. 3. Experimental coordinate system.

RESULTS AND DISCUSSION

The results are described in terms of the angles shown in Fig. 3. The specimen plane is defined as the yz plane with the current direction as the z axis. The Hall field is then measured along the y axis, and the magnetic field is in the xy plane. Logan and Marcus[1] express their results in terms of the polar coordinates of the hexad axis (α,β), but it is more convenient to express the Hall field E_y in terms of the angles ϵ and δ.

$$E_y/-j=\{R_2\cos^2\epsilon+R_1\sin^2\epsilon\}B_x + \{\tfrac{1}{2}(R_1-R_2)\sin 2\epsilon\sin\delta\}B_y + \{\tfrac{1}{2}(R_1-R_2)\sin 2\epsilon\cos\delta\}B_z. \quad (6)$$

If the system is correctly aligned, $B_z=0$ and E_y is then

TABLE II. Hall coefficients R_H (10^{-12} Ω cm G^{-1}), single crystals.

	Zn (297°K)		Zn (77°K)		Cd (297°K)	
	R_1	R_2	R_1	R_2	R_1	R_2
1	1.4	−0.14			1.34	0.32
2	1.7	−0.32	2.3	+0.28	1.43	0.29
2′	1.4	−0.32				
3	1.8	−0.33	2.2	+0.21	1.43	0.39
4	1.6	−0.30			1.30	0.46
5	1.3	−0.26			1.36	0.34
6	2.5	−0.23			1.46	0.42
7	1.9	−0.14	1.8	+0.29		
8	1.4	···				
Best value	1.4	−0.28	1.8	+0.28	1.39	0.39

[6] B. D. Cullity, *Elements of X-Ray Diffraction* (Addison-Wesley Publishing Company, Inc., Reading, Massachusetts, 1956), p. 290.

a sinusoidal function of the magnet azimuth θ. The extrema of the sine curve are displaced from the positions $\theta=\pi/2$, $\theta=3\pi/2$, which they would occupy for an isotropic material by the angle ψ, where

$$\cot\psi=(R_2\cos^2\epsilon+R_1\sin^2\epsilon)/\{\tfrac{1}{2}(R_1-R_2)\sin 2\epsilon\sin\delta\}. \quad (7)$$

The Hall coefficients R_1 and R_2 can be most conveniently determined from the experimental values of $E_y(0)$ and $E_y(\pi/2)$; or alternatively, from $E_y(\max)$ and ψ. The results obtained are listed in Table II.

The errors in the values of R_1 and R_2 determined in this way arise in various ways. These can be divided into two groups:

(a) Errors in determination of the electrical quantities j, E_y, and B. These errors are small and reasonably

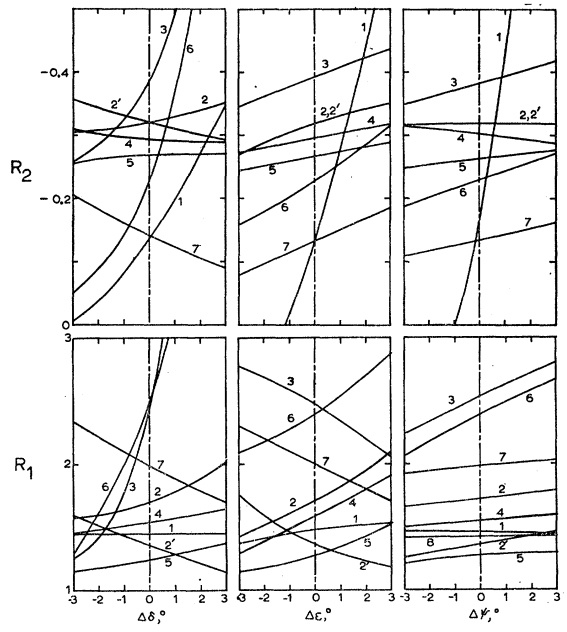

FIG. 4. The effect of angular errors on R_1 and R_2: zinc.

constant in these experiments. The absolute errors introduced are probably not greater than $\pm 2\%$; the relative scatter is considerably less.

(b) Errors in determination of the geometrical quantities:

(i) The polar coordinates of the hexad axis relative to the specimen geometry. These angles are probably not more accurately defined than $\pm 1°$ by the Laue method.

(ii) The angle between the current direction and the Hall probes and other possible skewness in the experimentally defined reference system in Fig. 3. These angles again may be in error by as much as 1°, although great care was taken to construct a rigid and accurately locating specimen holder mounting.

(iii) The angle ψ. It is difficult, even with the precise

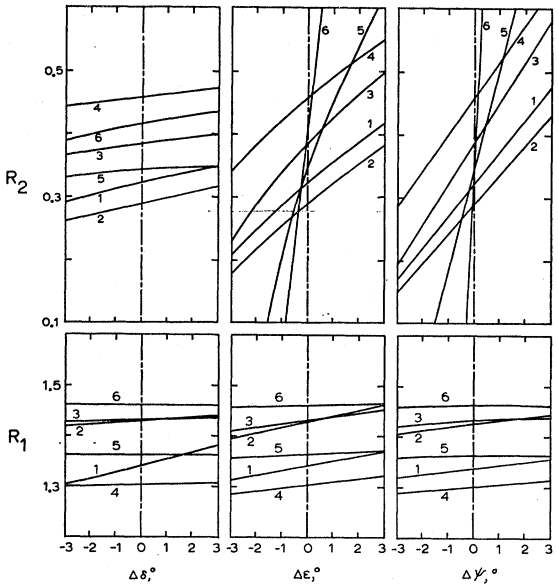

FIG. 5. The effect of angular errors on R_1 and R_2: cadmium.

data obtained in these experiments, to locate the position of the maximum on the sine curve to better than 2°.

The effect of the angular errors on the measured values of R_1 and R_2 are difficult to estimate. In Figs. 4 and 5 are shown graphs of the variation of R_1 and R_2 for both metals with ϵ, δ, and ψ separately about the experimentally determined values. It can be seen that within the experimental definition of these angles the variation in the coefficients is large. As a measure, in Figs. 6 and 7 are shown the bandwidths of results as a function of an "error angle" ϕ. Since ψ is less well defined than the other quantities, it has been assumed that $\Delta\epsilon=\Delta\delta=\phi$; $\Delta\psi=2\phi$. The sign of the error has been chosen to minimize the bandwidth, and it can be seen that in fact the bandwidth becomes zero for values of ϕ less than the 1° possible estimated on experimental grounds. However, the fact that crystals for which R_1 or R_2 vary

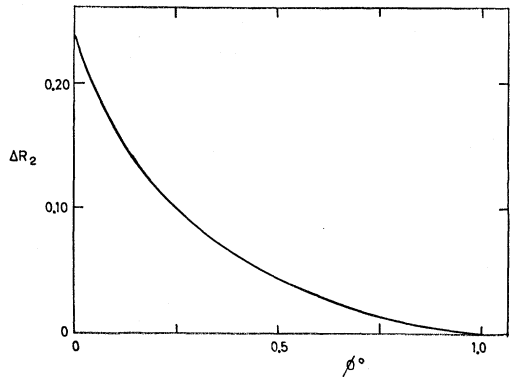

FIG. 6. Effect of combined angular errors on the range of R_2 zinc at room temperature.

very rapidly with some of the angles nevertheless give values close to those obtained for the other crystals, suggests that the angles were actually more accurately determined than the estimates above would suggest. No cadmium crystals were grown for which the basal plane was very far from the plane of the sheet. Consequently, the observed Hall signal was nearly all due to R_1, which varies only slightly with ϵ, δ, and ψ. The observed results, as listed in Table II, show that all the values of R_1 lie within $\pm 5\%$ of the mean. It seems likely, therefore, that this is the order of the scatter in the data due to sources other than angular variations. The existence of errors other than angular errors is confirmed by the difference between the results 2 and 2′ for zinc. It is impossible to reconcile R_1 and R_2 for these two results by any choice of ϵ, δ, and ψ, although, in fact, these results were obtained from the same specimen, simply removed from the mount and rotated through 180° before remeasurement. On these grounds, it is felt that probably the weighted mean value of the larger component R_1 is within 20% of the true value. These weighted mean values are shown in Table II. All these experiments were performed at 297°K. A limited number of measurements were performed on zinc single crystals at 77°K, and the mean of these results is also shown in Table II. The agreement with the results of Logan[1] and of Noskov[5] shown in Table I is very good. It is interesting to note that the sign of the smaller component R_2 changes between 297 and 77°K.

THE EFFECT OF ANNEALING THE SINGLE CRYSTALS

In spite of the care taken to avoid stressing the crystals, it was thought that during preparation and mounting of the specimens some deformation must have taken place. The effect of annealing the entire specimen assembly at 100°C was therefore studied. In the main, the value of the Hall signal increased with annealing time, reaching a constant value after about 24 h. In some cases, however, the signal *decreased* to a steady value, and in others there was no significant change. In all cases the total change was not greater than 10%. There was no obvious correlation between the type of behavior and the orientation of the crystal. This effect is interesting and needs further study. For the majority of the experiments described in this paper the specimens were annealed at 100°C for 48 h to permit the Hall signal to reach its steady value.

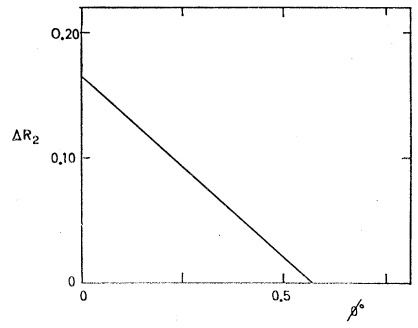

FIG. 7. Effect of combined angular errors on the range of R_2 cadmium at room temperature.

POLYCRYSTALLINE SAMPLES

The application of single-crystal results to the interpretation of polycrystalline specimens requires three assumptions:

(1) The grain boundaries do not make a significant contribution to the Hall effect. This is probably justified, since in high-purity metals with large grain size, the amount of material whose properties are affected by the grain boundaries is small.

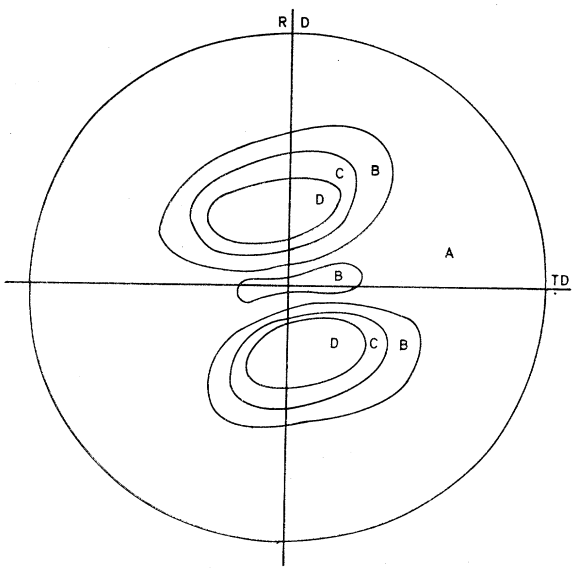

FIG. 8. (0001) pole figure for rolled zinc. Pole density increases from A to D.

(2) The short circuiting of the specimen current by crystals, with their low resistivity direction parallel to the current, is insignificant. In zinc, the difference between the two components of the resistivity is approximately 5%. For an ideal specimen consisting of two equally sized crystals connected only at their ends, one with the hexad axis normal to the current, the other with the hexad axis parallel to the current, the Hall coefficient calculated, allowing for the difference in the current in each crystal, is approximately 4% greater than the value calculated, assuming the current density in each crystal is the same. For a real situation the difference will be much less.

(3) The short circuiting of the Hall field is small. It is much more difficult to evaluate the effect of the short circuiting of the Hall signal in adjacent grains, because of the multiple connection of the circuit. Loop currents

will flow as a result of the differences in Hall potential, but it is not possible to calculate the magnitude of the consequent alteration in the net Hall voltage. It seems likely that the effect of the short circuiting will be to reduce the apparent Hall voltage, and there is no *a priori* reason for supposing that the effect is negligible.

If these three assumptions are made, then one can simply sum the contributions to the total Hall signal of all the grains, treating each as a separate single crystal. Equation (6) then becomes

$$E_y=-j\{\sum_{\epsilon=0}^{\pi/2}(R_2\cos^2\epsilon+R_1\sin^2\epsilon)n(\epsilon)B_x$$
$$+\tfrac{1}{2}\sum_{\epsilon=0}^{\pi/2}\sum_{\delta=0}^{2\pi}(R_1-R_2)\sin 2\epsilon\sin\delta n(\epsilon)n(\delta)B_y\}\,, \quad (8)$$

where $n(\epsilon)$ and $n(\delta)$ are normalized weighting functions

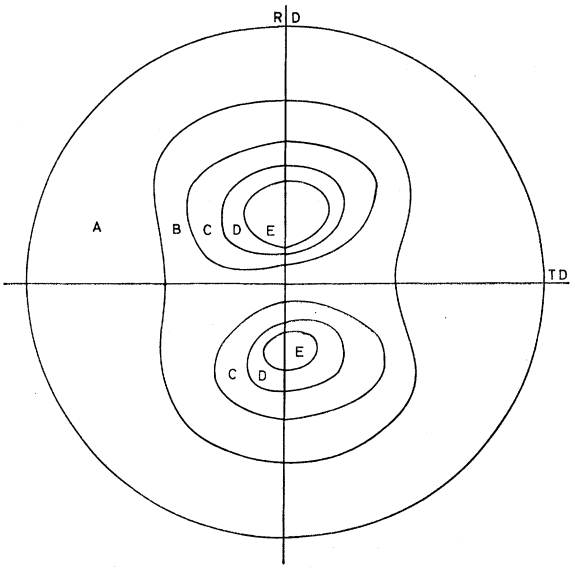

FIG. 9. (0001) pole figure for rolled cadmium. Pole density increases from A to E.

representing the distribution of (0001) poles as a function of ϵ and δ. These functions can be determined from the pole figure, or, more properly, from the x-ray data used to plot the pole figure. If the pole figure possesses a twofold rotation axis of symmetry normal to the plane of the sheet, so that

$$n(\delta)=n(\delta+\pi)$$

or a mirror line parallel to the current so that

$$n(\delta)=n(-\delta)\,,$$

the second term in (8) sums to zero since it contains the term

$$\sum_{\delta=0}^{2\pi}n(\delta)\sin\delta.$$

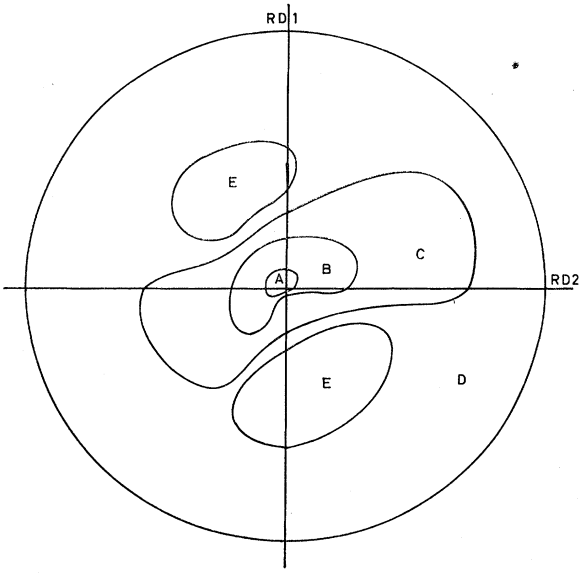

FIG. 10. (0001) pole figure for cross-rolled zinc. Pole increases from A to E.

Consequently, the extrema of $E_y(\theta)$ will occur at $\theta=\pi/2$ and $\theta=3\pi/2$, exactly as for an isotropic material. This is, in fact, found experimentally for all the polycrystalline specimens examined in this investigation to within $\pm 2°$. The Hall coefficient is then

$$R_H=\sum_{\epsilon=0}^{\pi/2}(R_2\cos^2\epsilon+R_1\sin^2\epsilon)n(\epsilon)$$

or

$$R_H=R_2\sum_{\epsilon=0}^{\pi/2}n(\epsilon)\cos^2\epsilon+R_1\sum_{\epsilon=0}^{\pi/2}n(\epsilon)\sin^2(\epsilon). \quad (9)$$

Specimens of various textures were produced for each metal. Figures 8 and 9 show the (0001) pole figures for rolled zinc and cadmium, respectively. Figures 10 and 11 show pole figures for zinc and cadmium after cross rolling. The slight asymmetry in all these pole figures is probably due to the rolls not being exactly parallel. Figures 12 and 13 show the weighting factors $n(\epsilon)$ as a function of ϵ for the two cadmium specimens. The integrated weighting functions and the calculated values of the Hall coefficient for the various specimens are listed in Table III, together with the observed values.

The calculated Hall effects for the zinc specimens are very close to the experimental results, but the results for cadmium are all smaller than the predicted value. R_1 is known with some accuracy for cadmium, and the difference in the weighting factors produced by the cross rolling is large. Although R_2 is much less well known, the value R_2 would have to be assigned to obtain agreement between prediction and experiment is altogether too low. It is felt, therefore, that the disagreement is significant and that the initial assumptions are invalid. If the second assumption is incorrect, the dif-

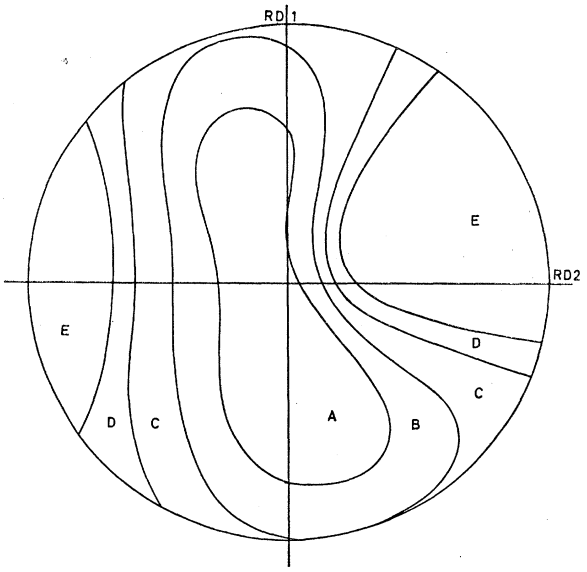

FIG. 11. (0001) pole figure for cross-rolled cadmium. Pole density increases from A to E.

ference between the predicted and observed results should have the opposite sign, but if the third assumption is incorrect the error introduced would be of the kind observed. Consequently, it seems likely that in cadmium the short circuiting of the Hall signal is not negligible.

In Table III are also shown the values of R_1 and R_2 calculated from specimens of different textures, together with the range of values consequent on a 10% error in the calculation of the integrated weighting factors. This is a larger error than is likely. The qualitative agreement with the values measured on single crystals is good, but because of the rather large scatter bandwidth consequent on the assumed error in the integrated weighting factor, the quantitative agreement is only fair.

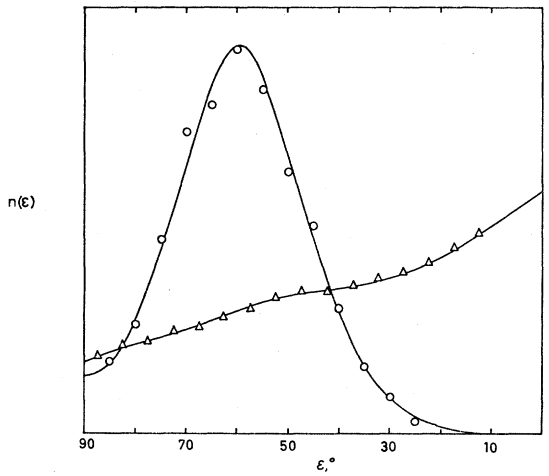

FIG. 12. Weighting factors for cadmium sheet. Circles cross rolled. Triangles straight rolled.

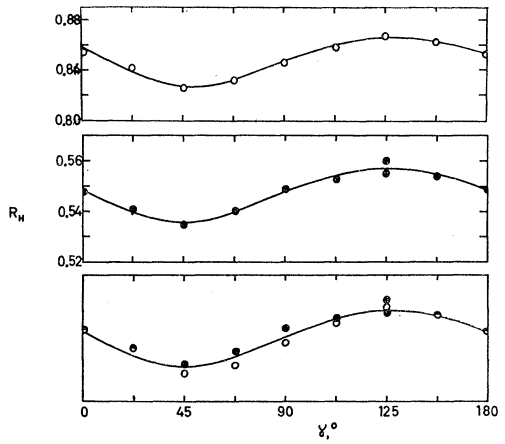

FIG. 13. The variation of R_H with γ the angle between the rolling direction and the z axis. Open circles Cd. Shaded circles Zn. The bottom graph is a normalized plot.

It seems, therefore, that only approximate values of the independent coefficients of the Hall vector can be obtained from polycrystalline samples. In part, this is due to the relatively small variation in the integrated weighting factors produced by considerable changes in the pole figure. An accurate result depends on obtaining textures which produce very different values for the integrated weighting factors. For the titanium problem studied by Roesch[4] this is not of such great importance, since both components of the Hall vector are large and of opposite sign.

THE EFFECT OF ROLLING DIRECTION

Equation (9) shows that R_H depends on ϵ only through the functions $\cos^2\epsilon$, $\sin^2\epsilon$, and $n(\epsilon)$. All of these functions are independent of γ, the angle that the rolling direction makes with the current density, so that it follows that the observed value of the Hall constant in sheet specimens should be independent of the angle at which the specimen is cut from the sheet. This has been checked for both zinc and cadmium. The results are shown in Fig. 14. The variation of the Hall coefficient is only 5% compared with an absolute experimental error (shown by the vertical bars) of approximately $\pm 3\%$, but as the normalized curves show, there does appear to be a systematic variation of R_H with γ, with a period of π. In addition, although the absolute accuracy is of the order of $\pm 3\%$, the relative accuracy of these observations is much better.

It is possible that this variation is due to a nonvanishing contribution by the B_y term in Eq. (8). This equation may be written

$$R(\theta)=\sum_{\epsilon} f_x(\epsilon)n(\epsilon)\cos\theta+\sum_{\epsilon\delta} f_y(\epsilon)n(\epsilon)\sin\delta n(\delta)\sin\theta,$$

where

$$f_x(\epsilon)=R_2\cos^2\epsilon+R_1\sin^2\epsilon,\quad f_y(\epsilon)=\tfrac{1}{2}(R_1-R_2)\sin 2\epsilon \quad (10)$$

TABLE III. Hall coefficients (10^{-12} Ω cm G^{-1}), polycrystalline material.

	Zn $4N$[a]	Zn $5N$		Zn $5NXR$[b]		Cd $5N$	Cd $5NXR$
	297°K	297°K	77°K	297°K	77°K	297°K	297°K
$\Sigma\, n(\epsilon)\cos^2\epsilon$	0.54	0.43		0.55		0.60	0.33
Predicted R_H	0.50	0.68	1.15	0.47	0.96	0.77	1.05
Range	±0.1	±0.1	±0.15	±0.1	±0.1	±0.1	±0.1
Experimental R_H	0.55	0.65	1.06	0.43	0.84	0.61	0.87
Calculated $\frac{R_1}{R_2}$		297°		77°		297°	
		1.44±0.50		1.85±0.70		1.20±0.4	
		−0.40±0.28		0.20±0.30		0.22±0.2	

[a] $4N$ refers to 99.99% and $5N$ to 99.999% pure material.
[b] XR signifies cross-rolled material.

and

$$B_x = B\cos\theta \quad B_y = B\sin\theta.$$

The measured value of R_H in the maximum of $R(\theta)$, i.e.,

$$R_H = \{[\sum_{\epsilon} f_x(\epsilon)n(\epsilon)]^2 + [\sum_{\epsilon\delta} f_y(\epsilon)n(\epsilon)\sin\delta n(\delta)]^2\}^{1/2}$$
$$= \sum_{\epsilon} f_x(\epsilon)n(\epsilon) \times \{1 + [\sum_{\epsilon\delta} f_y(\epsilon)n(\epsilon)\sin\delta n(\delta)]^2 / [\sum_{\epsilon} f_x(\epsilon)n(\epsilon)]^2\}^{1/2}. \quad (11)$$

If

$$\sum_{\epsilon\delta} f_y(\epsilon)n(\epsilon)\sin\delta n(\delta) \ll \sum_{\epsilon} f_x(\epsilon)n(\epsilon), \quad (12)$$

Eq. (11) becomes

$$R_H = \sum_{\epsilon} f_x(\epsilon)n(\epsilon) \times \{1 + \tfrac{1}{2}[\sum_{\epsilon\delta} f_y(\epsilon)n(\epsilon)\sin\delta n(\delta)]^2 / [\sum_{\epsilon} f_x(\epsilon)n(\epsilon)]^2$$
$$= \sum f_x(\epsilon)n(\epsilon) + [\sum_{\epsilon\delta} f_y(\epsilon)n(\epsilon)\sin\delta n(\delta)]^2 / 2\sum_{\epsilon} f_x(\epsilon)n(\epsilon). \quad (13)$$

But if the contribution of the B_y term in (8) vanishes,

$$R_H = R_H{}^0 = \sum_{\epsilon} f_x(\epsilon)n(\epsilon). \quad (14)$$

The contribution of the B_y term may then be written as $R_H{}^1$, so that

$$R_H = R_H{}^0 + R_H{}^1,$$

where

$$R_H{}^1 = [\sum_{\epsilon,\delta=0}^{\epsilon=\pi/2,\delta=2\pi} f_y(\epsilon)n(\epsilon)\sin\delta n(\delta)]^2 / 2R_H{}^0. \quad (15)$$

The condition (12) is equivalent to the condition that $R_H{}^1 \ll R_H{}^0$, which is justified experimentally. Equation (15) may be written

$$R_H{}^1 = K(\epsilon)\{\sum_{\delta} \sin\delta n(\delta)\}^2, \quad (16)$$

where now $K(\epsilon)$ is a function of ϵ only, independent of δ.

The term $\sum \sin\delta n(\delta)$ will have opposite signs for $0<\delta<\pi$ and for $\pi<\delta<2\pi$. The condition that this term is zero is then that the magnitude of the sum on either side of the axis $\delta=0$ is equal. This is plainly true if there is a twofold axis of symmetry normal to the sheet, and is also true if the line $\delta=0$ is a mirror line. For pole figures in this investigation there is a mirror line approximately parallel to the rolling direction, so that for specimens cut with their long axis parallel to the rolling direction ($\gamma=0$) the summation above is zero and consequently $R_H{}^1=0$. However, for $\gamma\neq 0$

$$\sum_{\delta=0}^{\pi} \sin\delta n(\delta) + \sum_{\delta=0}^{2\pi} \sin\delta n(\delta) \neq 0, \quad (17)$$

and, consequently, $R_H{}^1\neq 0$. The magnitude of the inequality (12) increases as γ approaches $\pi/2$, since the regions of high $n(\delta)$ are thus rotated into regions where the magnitude of $\sin\delta$ has its maximum value. The magnitude of the inequality (12) has a periodic variation with γ of period π, although the absolute value varies with γ with a period 2π. However, $R_H{}^1$ is related to the square of the inequality (12), and thus will show a periodic variation with the angle between the rolling direction and the current direction with a period of π, in agreement with the observed behavior. A detailed calculation would require values for the function $K(\epsilon)$ and the function $n(\delta)$. While this is possible, the errors involved in an experimental determination of the functions would be larger than the magnitude of $R_H{}^1$.

CONCLUSIONS

The two independent coefficients of the Hall vector for zinc and cadmium have been measured for single-

crystal specimens. These values have been used to predict the Hall coefficient for polycrystalline samples, and the possibility of using polycrystalline specimens to determine the independent coefficients has been investigated. It is concluded that good quantitative values will only be obtained if it is possible to obtain specimens with very different textures.

ACKNOWLEDGMENTS

This work was supported by a grant from the Department of Scientific and Industrial Research. One of the authors (G.S.L.) wishes also to acknowledge receipt of a D.S.I.R. Research Studentship. Thanks are also due to Dr. G. T. Higgins for assistance in determining the pole figures.

PHYSICAL REVIEW VOLUME 135, NUMBER 4A 17 AUGUST 1964

Spin-Lattice Relaxation in Free-Radical Complexes

KRISHNAJI AND B. N. MISRA
Department of Physics, Allahabad University, Allahabad, India
(Received 17 March 1964)

Spin-spin and spin-lattice relaxation times have been determined at 19.3 Mc/sec for samples of 1,1-diphenyl-2-picrylhydrazyl, picryl-*N*-aminocarbazyl, and their recrystallized samples from various solvents. It is found that the spin-lattice relaxation time increases in most of the recrystallized samples and the melting points of the samples decrease. It has been possible to explain these results in terms of variable exchange interaction due to a possible change in lattice. The three-reservoir model of Bloembergen and Wang has been used in order to evaluate the relaxation times for spin to exchange and exchange to lattice.

INTRODUCTION

IN solids, spin-lattice relaxation time gives valuable information regarding the structure of the lattice and spin-orbit coupling. Though in free radicals, the spin-orbit coupling is weak and spin-lattice relaxation time is usually large, yet it has been found possible to determine it by measuring the linewidth for two values of the radio-frequency fields.

We have determined T_1 and T_2 the spin-lattice and spin-spin relaxation times for 1,1-diphenyl-2-picrylhydrazyl, picryl-*N*-aminocarbazyl, and their recrystallized samples from various solvents. The melting points of the samples have also been determined for all the cases. It is found that increase in spin-lattice relaxation time is accompanied by a decrease in melting point. A large change in spin-lattice relaxation time is not necessarily accompanied by a large change in linewidth. It has been possible to explain these results in terms of possible change in lattice. The three-reservoir model of Bloembergen and Wang[1] has been used in order to evaluate the relaxation times from spin to exchange and exchange to lattice.

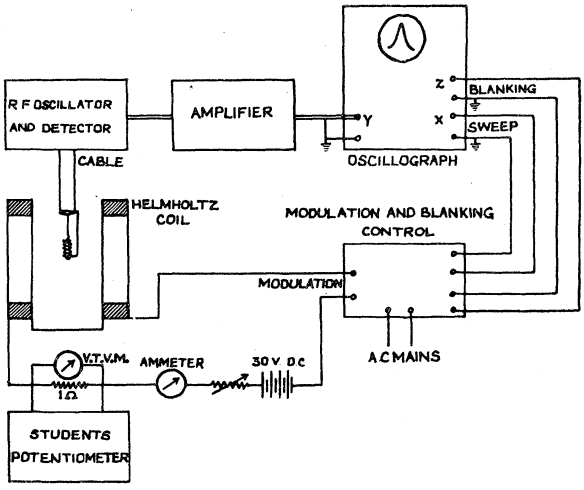

FIG. 1. Block diagram of electron spin resonance rf setup.

EXPERIMENTAL TECHNIQUE

An rf electron spin-resonance spectrometer at 19.3 Mc/sec using a Clapp-type oscillator and detector, shown in Fig. 1, has been used here for this work. The sensitivity is sufficiently high when it is oscillating weakly, and the method is found to be most convenient for this measurement. The spin-spin relaxation time T_2 and spin-lattice relaxation time T_1 have been determined by measuring the half-linewidth between half-maximum points, and for two values of the rf magnetic fields H_1 and H_2, respectively. The expressions for the half-linewidth derived from the Bloch[2] equations are as follows:

$$\delta_1=[1+(\gamma H_1)^2T_1T_2]^{1/2}/\gamma T_2, \quad (1)$$

$$\delta_2=[1+(\gamma H_2)^2T_1T_2]^{1/2}/\gamma T_2, \quad (2)$$

where $\gamma=g\beta/\hbar$. The expressions for T_1 and T_2 can be written by squaring and rearranging the Eqs. (1)

[1] N. Bloembergen and S. Wang, Phys. Rev. **93**, 72 (1954).
[2] F. Block, Phys. Rev. **70**, 460 (1946).